Video Article

Automated Detection and Ablation of Neurons *In vitro* using Ultra-fast Laser **Technology**

John A. Hayes¹, Xueying Wang¹, Christopher A. Del Negro¹

¹Department of Applied Science, The College of William and Mary

Correspondence to: Christopher A. Del Negro at cadeln@wm.edu

URL: http://www.jove.com/video/2193

DOI: doi:10.3791/2193

Keywords: central pattern generation, central pattern generator, rhythm generation, calcium indicators, two-photon microscopy, lesion, ablation

Date Published: 6/15/2015

Citation: Hayes, J.A., Wang, X., Del Negro, C.A. Automated Detection and Ablation of Neurons In vitro using Ultra-fast Laser Technology. J. Vis.

Exp. (), e2193, doi:10.3791/2193 (2015).

Abstract

Lesioning is one of the most powerful tools in systems neuroscience. It allows one to test the role of particular cells by removing them from a neural circuit via ablation, and then assessing the effect on network function. However, the level of new knowledge these lesion experiments yield depends on the selectivity and accuracy of the lesion.

Here we present a novel approach consisting of automated cell-specific two photon laser-ablation experiments performed in vitro in the context of network function. We developed a computer-controlled system to detect neurons via multi-photon microscopy, store their locations in memory, and then laser-ablate the target neurons one at a time, in sequence, while monitoring the output of the neural circuit electrophysiologically. Use of a long-wavelength pulsed laser provides unprecedented specificity and control of the lesion in 3D, which we argue will provide equally powerful new insights.

Our investigations focus on the circuit properties of the preBötzinger Complex (preBötC) the respiratory central pattern generator located in the lower brainstem of humans and all mammals (1,2). Retained in thin slice preparations from neonatal rodents, the preBötC spontaneously generates inspiratory motor rhythms that are measurable in vitro. Selective serial lesions can therefore be performed in the context of fictive breathing behavior.

The experimental approach we describe will elucidate the cellular composition of the preBötC and thus provide significant new information regarding the generation and control of breathing. Subsequent applications of this technique to other systems will enable other groups and investigators to interrogate locomotor and masticatory CPGs that can be also be studied in spinal cord and hindbrain preparations in vitro. Indeed, our system will be broadly applicable to studying networks in vitro from any brain region.

Protocol

In vitro studies of breathing. The neural control of breathing was originally studied in vivo, using anesthetized cats and rabbits (4,5). However, since the isolated neonatal rodent brainstem can generate inspiratory motor patterns in vitro (6,7), newborn rats and mice have become important experimental models. The neonatal mouse slice preparation is particularly advantageous because it exposes the preBötC for imaging, electrophysiology, and laser ablation, while generating inspiratory motor patterns (1,2,8). And useful genetic models are frequently available for

Dissection and preparation of slices.

The Institutional Animal Care and Use Committee at The College of William & Mary approved the following protocols. Neonatal mice (P0-5) are anesthetized and dissected in ACSF (see Materials above). We use WT C57BL/6 mice, Dbx1LacZ knock-in mice (9), Dbx1ER-Cre (10), ROSA26^{LoxP-STOP-LoxP-EYFP} mice (i.e., R26^{EYFP}) and Ptf1a^{Cre} mice (11,12). The neuraxis is isolated and pinned with its ventral surface facing out onto a paraffin-coated paddle. The paddle is fixed into the vise of a vibrating microtome for sectioning in the transverse plane. We cut 300-550µm-thick transverse slices with the preBötC at the rostral surface, according to a calibrated atlas (8). The slices are mounted in a recording chamber and perfused with 27°C ACSF at 4 ml/min. The external potassium concentration ([K⁺]_o) is raised to 9 mM and inspiratory motor output is recorded from hypoglossal (XII) nerve roots (see Electrophysiology below.

Multi-photon and confocal microscopy.

A fixed-stage upright laser-scanning confocal microscope (Zeiss LSM 510) is equipped with three confocal visible-wavelength lasers and a tunable (720-980 nm) ultra-fast, mode-locked Ti:Sapphire laser, which generates 100-fs pulses at max 1.5 W (Mai Tai, Spectra Physics) for a final output of ~900 mW at 800 nm. A 120 W metal halide lamp (X-Cite 120, EXFO) is also used in some experiments for rapid screening of the tissue using fluorescent illumination. The LSM 510 scan head contains three internal descanned detectors, two external non-descanned detectors, one sub-stage descanned detector for bright-field and IR-DIC imaging, and a 12-bit cooled charge-coupled device camera for IR-DIC videomicroscopy in real time applications to position slice and electrodes (Axiocam). The robotic XY translation stage (Siskiyou Corp.) is used



to adjust the position of the slice preparation, in particular to move the imaging plane between bilaterally distributed regions of the preBötC. The robotics can be manually controlled for defining the XY domain of the bilaterally distributed preBötC, and then switched to computer control for uni- or bilateral serial ablations via Ablator.py.

Fluorescent labeling of Dbx1+ neurons.

We cross WT and Dbx1^{LacZ/+} mice to obtain viable heterozygous pups in Mendelian ratios, from which we cut slice preparations as described above. Slices are incubated in ACSF containing 1.5 mg/ml FDG for 30 min at 37° C. The lacZ gene product -galactosidase (gal) activates fluorescein and enables Dbx1⁺ neurons to be identified via fluorescence. We also cross Dbx1^{ER-Cre} and R26^{EYFP} mice to obtain Dbx1^{ER-Cre};R26^{EYFP} pups in which the timing of tamoxifen administration during pregnancy produces fluorescent Dbx1⁺ neurons in the preBötC and contiquous dorsomedial medulla.

Fluorescent labeling of Ptf1a+ neurons.

The Hox gene Ptf1a controls the development of glycinergic neurons that originate in the dorsal neural tube (11,12) and settle in the hindbrain preBötC area. Reporter gene expression in Ptf1a^{Cre};R26^{EYFP} mice is robust in the preBötC.

Loading Ca²⁺-sensitive fluorescent dye.

Incubate slice in 1.5 ml centrifuge tube with 100 µL of 9 mM K⁺ ACSF. Add 10 µL D-Mannitol stock solution (1 M) to the centrifuge tube. Thaw one aliquot of Fluo-8L AM stock solution and add its contents to centrifuge tube; the final Fluo-8L AM loading concentration is ~32 µM. Incubate the slice for 1.5-2 hours at room temperature (or 37° C in the dark). After incubation, rinse slice in normal 9 mM K⁺ ACSF in the recording chamber for 20-30 min while recording XII output, which should be stable in frequency and amplitude before beginning the experiment.

Electrophysiology.

XII nerve roots are recorded using suction electrodes and the differential amplifier. XII output is full-wave rectified and smoothed for ease of display. Most lesion experiments are done without intracellular recordings, but this additional form of measurement can be performed in conjunction with the detection and lesion experiment. We perform patch-clamp electrophysiology either with a current-clamp amplifier or using a patch-clamp amplifier in voltage- or current-clamp mode. All electrophysiology data are digitally acquired at 2-10 kHz using a 16-bit AD converter after analog 1 kHz filtering.

Define XY domain of target nucleus.

With the experimenter controlling the stage and focus, the slice is maneuvered to situate the preBötC in the center of the field of view under videomicroscopy. The GUI in XYTranslator_control. is used to save the coordinates of the center position, which becomes the definition of the center of the preBötC. Perform this localization on both sides of the transverse slice to define the preBötC bilaterally.

Define Z domain of target nucleus.

Again with the experimenter controlling the stage and focus, the slice is scanned with the configuration fluo-4-MP or YFP3 (as appropriate depending on the specimen slice) using the 20x objective and digital zoom to image the preBötC at cellular resolution. The user defines the depth (z-range) of the field on each side, and also defines the center point of the field bilaterally such that it is contained within 425 μ m2 (512x512 pixels). The z-values are entered into. POSITION_1_ZRANGE = [z_1 , z_2], POSITION_2_ZRANGE = [z_3 , z_4], in AblatorConfiguration.py where zi indicates confocal plane depth in μ m. This information is stored in memory so that robotics can translate the stage to Position 1 and 2 automatically.

Initialize hardware.

This step creates directories to store all the data, establishes connections to the robotic XY stage translators and microscope controller, and time syncs the computers.

Detect targets.

Neurons subject to the ablation protocols are either static, i.e. Dbx1⁺ or Ptf1a⁺, or dynamic, i.e. rhythmically active inspiratory neurons detectable via Ca²⁺ imaging.

Static targets are detected by an iterative threshold-crossing routine. The program acquires a high-resolution confocal image at a given depth (z-axis). Then an analysis feature in ImageJ finds a mask of local maxima. At first, with a high threshold, few local maxima are detected and the mask is small and sparse with regions of interest (ROIs). The routine then lowers the threshold by a user-defined increment and re-analyzes the image. As threshold decreases in steps, more ROIs become detectable. These newly detected ROIs are added to the mask, which results in an expansion of the list of potential target neurons. The threshold is decreased incrementally over a user-defined number of iterations, which generally entails 100-200 partitions up to 4096 values of fluorescence intensity (for a 12-bit image). As the detection process continues and threshold decreases incrementally, the smaller ROIs from prior iterations which are fully contained in larger ROIs from the current iteration are discarded, and the new larger ROIs are retained. Conversely, when a newly detected ROI at the current iteration envelopes two or more ROIs

from a prior iteration, the newly detected 'superset' ROI is discarded, and the multiple ROIs from the earlier iteration are retained. After looping through all the partitions, the final set of ROIs is saved as the mask of target neurons for that focal plane (measured according to z-axis position). The process described above is repeated throughout the z-axis on both sides of the slice preparation. We generally move in 10-µm increments in the z-axis. The final set of targets is stored in memory.

Dynamic targets are also detected with an iterative threshold-crossing algorithm as described above. However, an additional layer of analysis is applied to evaluate rhythmicity. Rather than take a single high-resolution confocal image, here the program takes a time series of images (50 ms per frame at 20 Hz). The stack of images is projected into one planar image by calculating the standard deviation (SD) of the fluorescence intensity, which should ideally indicate regions whose fluorescence changes periodically during the acquisition phase. This first stage of processing thus produces the mask of targets based on an indirect measure of rhythmicity. Once the mask of ROIs is determined for dynamic targets, the program analyzes each ROI to assess dynamic fluorescence changes from the time series. A temporal lag filter is applied to obtain Δ F/F for each ROI using scripted routines in ImageJ, which can be plotted as a function of time or as colored-coded rasters for multiple ROIs (Fig. 10, right column). The program then calculates a relative power spectrum density graph for each ROI using Fourier analysis, and searches for significant power at frequencies in the range of 0.2-0.35 Hz, which is typical for respiratory rhythm in breathing slice preparations. (Other users in different preparations could adjust the appropriate frequency in this step.) A score is evaluated based on the relative peak power in this frequency range. ROIs that fail to score at least 40 (arbitrary units) are discarded. In this way, the dynamic target selector arrives at a final array of target neurons, in which many of the original static ROIs are no longer considered bona fide respiratory neurons. The process of finding rhythmically active respiratory neurons in each confocal section is repeated throughout the z-axis, and bilaterally repeated. The final set of rhythmic, i.e., dynamic, targets is stored in memory.

Step 4: Choose target.

Selecting a target for ablation is random by default, drawn from the 3D volume of detected neurons (Dbx1+ or inspiratory) as defined by static or dynamic criteria. For example, the upper graphs in Fig. 7 show 42 random selections [right] from 233 possible targets [left]. However, selection criteria can be based on any quantifiable measure, for example:

- 1. Centroid: preferential selection based on proximity to the center of collected targets,
- Magnitude of fluorescence: the magnitude of the ΔF/F can be used to preferentially lesion the strongest rhythmically active inspiratory neurons first.
- 3. Left-right alternation: before the lesioning loop begins, the user can define whether to alternate 1-to-1 lesions across bilateral parts of the preBötC or to perform n-number of lesions ipsilaterally before switching to the contralateral side.

Ablation.

The Ti:Sapphire laser is tuned to 800-810 nm, focused on the target ROI in a planar scan mode but with maximum optical zoom, and then scanned with maximum intensity over the soma of the target until the software deems it vaporized. Confirmation of target ablation is obtained by imaging the ROI using the descanned detector on the laser-scanning microscope with a 560-615 nM band-pass filter. Emission within this range detects light scattering due to vaporized tissue (i.e., a cavity in the tissue now filled with water vapor), while excluding green dyes (e.g., fluorescein, Fluo-8L, etc...) as well as IR wavelength reflections from the laser. The multi-photon approach is inherently confocal so there is no photo-damage outside the focal plane. The Ablation is repeated according to the strategy (see 3.b.viii in SOFTWARE, above) until all targets are exhausted.

The network activity will have been recorded throughout the experiment, so the effects of lesions can be monitored in real time, and by post-hoc analysis of the time course of the experiment. The software writes a log file that documents the progress of the experiment and logs all lesions by index number. It also records images of each lesioned ROI and obtains images every n-lesions according to the environment variable annotateEveryXLesions = 10, which is here set to its default of 10.

Post hoc histology tests of slices subject to lesion protocols. We use a calibrated atlas by to verify that the preBötC was at the slice surface (8). This atlas was originally for rats, but has been expanded to include mice, and the authors have generously provided us with a preprint for our use in mice. After the lesion experiment, the slice is placed into fixation solution composed of 4% paraformaldehyde in phosphate buffer (1:2 mixture of $0.1 \text{ M NaH}_2\text{PO}_4 + 0.1 \text{ M Na}_2\text{HPO}_4$ in H_2O , pH = 7.2) for 1 hour. The slice is then rinsed in phosphate buffer for 2 min. After rinsing, the slice is submerged for 45-60 sec in Staining solution. The slice is then washed in a series of ethanol solutions (8). Finally, the slice is mounted in a well slide for bright field microscopy, photographed via digital CCD, and measured against the calibrated atlas for anatomical landmarks.

Discussion

Breathing consists of periodic movements of the diaphragm, thorax, and airways that result in ventilation. The underlying motor pattern originates in the brainstem. A contiguous ventrolateral column of respiratory neurons extends from the facial motor nucleus (VII) of the hindbrain to the phrenic motor nucleus (C3-C5) of the spinal cord. This column produces the coordinated motor pattern in living animals (4), bur there are functionally significant distinctions among the constituent respiratory neurons and nuclei. In particular, propriomedullary interneurons in the preBötC specialize in rhythm generation (2,13-15).

But which preBötC neurons are rhythmogenic? Approximately 50% of neurons in the preBötC are glycinergic (16), yet inhibitory neurotransmission is not obligatory for respiratory rhythm generation (14,17-19). Glutamatergic neurons are known to be essential for rhythmogenesis (20-24), but peptidergic systems appear to be important as well. Neuropeptides including thyrotropin releasing hormone (TRH), tachykinin substance P (SP), and somatostatin (SST) act in the preBötC to vigorously modulate respiratory frequency (14,25-33). It is possible that neurons (or subsets of neurons) that have until recently been distinguished by peptidergic or glutamatergic transmitter phenotypes may in fact map to genetically distinct interneuron lineages, which has been demonstrated in the spinal locomotor networks (34,35). These

genetic lineages can be labeled using a variety of fluorescent reporters, and then targeted in laser ablation experiments such as we have here developed. Transcription factor Dbx1 may provide a particularly attractive genetic origin for the rhythmogenic kernel in the preBötC, if it gives rise to peptide-sensitive and glutamatergic neurons, which co-release SST (9,12), but this has yet to be demonstrated in hindbrain. Thus we initiated the protocols here to test this idea via Dbx1+-selective cell ablations in the context of network function in vitro.

Two experiments that tested the cellular make up of the rhythm-generating kernel *in vivo* provide rationale for the present project. Injections in the preBötC of the ribosomal toxin saporin conjugated to SP killed NK1R+ neurons over several days. Freely behaving adult rats showed a progressive diminution of breathing behavior that led inexorably to ataxic breathing, respiratory pathology, and death (13,36). In another experiment, transiently silencing SST+ neurons in the preBötC via the K⁺ channel-coupled allatostatin receptor caused reversible apneas in vivo, in which the animal subjects had to be mechanically ventilated to prevent asphyxiation (until the effects of allatostatin washed out) (15). These experiments demonstrated the existence of an essential core of glutamatergic neurons in the preBötC that are either SST+ or NK1R+. However, the extent to which these neuropeptide receptor-expressing neurons reflect the same or overlapping subpopulations remains unknown. Thus, the cellular composition of the preBötC has not been unambiguously evaluated. Moreover, the cellular-level mechanisms that led to ataxic breathing and central apnea in the experiments above could not be quantified in vivo, which limits the interpretability of the data.

Two overarching questions remain unsolved: 1) Which neurons comprise the rhythmogenic core and how can we properly characterize them? And, 2) how do graded lesions impact rhythm-generating capability and what might this progression cell loss teach us about disease?

Each marker in the experiments described above (i.e., NK1R vs. SST) identifies a key fraction of the preBötC, but neither marker is definitive. NK1R+ and SST+/SST2aR+ neurons reflect distinct but overlapping subpopulations in the preBötC (29, Figs. 2 and 3). Dbx1+ neurons in the spinal cord are glutamatergic and settle in the ventrolateral region of the gray matter. Their position in hindbrain is similar. If the Dbx1+ neurons have a similar transmitter phenotype, and are peptide-sensitive as well as peptide-sensitive, then Dbx1 may define a superset of rhythmogenic neurons. We are actively testing whether Dbx1+ neurons comprise the rhythmogenic kernel of the preBötC using the laser lesion approach described here.

Determining the cellular composition of the preBötC is a critical problem for basic respiratory physiology and neuroscience, with important ramifications for public health. Adult rats subjected to chronic saporin lesions provide a model of respiratory failure with a central etiology (13), which often occurs in the elderly and in patients suffering neurodegenerative disorders such as multiple systems atrophy (MSA) (37,38) and Parkinson disease (39). However, these experiments could not measure how progressive loss of preBötC neurons correlates with deteriorating respiratory function. Thus the cellular mechanisms that lead to pathophysiology remain incompletely understood. Additionally, activating allatostatin receptors *in vivo* transiently silences a large fraction of the preBötC at once, which precludes studying the effects of graded neuron removal altogether. While wholesale silencing and chronic lesion experiments *in vivo* provided important new knowledge, both have limitations as disease models. We propose to overcome some of these limitations, and provide an important complement to *in vivo* approaches, by performing graded cell-specific lesions in an *in vitro* slice model of breathing. Neurons in the preBötC will be precisely identified by fluorescent markers (Dbx1-specific or rhythmic Ca²⁺ activity) and then ablated in a controlled sequence. We are able to quantify the effects on inspiratory motor output (XII discharge) as a function of number of cells destroyed in the preBötC.

Thus this lesioning method may help elucidate the mechanisms contributing to respiratory failure in MSA and Parkinsonism. This *in vitro* approach will also provide a model that may be broadly applicable to understanding neonatal breathing disorders such as apnea of prematurity, and could be readily adapted using serotonergic neuronal markers to study sudden infant death syndrome (SIDS) (40). Our *in vitro* approach will also provide basic information that may help to understand diverse respiratory pathologies that impact sleep including central sleep apnea and catathrenia, a.k.a. nocturnal groaning (41) among other forms of sleep-disordered breathing (36). Neurons with low endogenous Ca²⁺ buffers including XII motoneurons and neurons in the preBötC (42) are susceptible to degeneration and cell death in amyotrophic lateral sclerosis (ALS) (43). Thus, we can also provide a complementary *in vitro* model of ALS in which either XII motoneurons or preBötC neurons can be selectively ablated in graded fashion.

Respiration, locomotion and ingestive oral-motor behaviors all consist of rhythmic movements formed by central pattern generator (CPG) networks of the brainstem and spinal cord (44,45). Understanding CPGs is an important problem in neurobiology that takes on added significance when considering the significant health problems that result from spinal cord and hindbrain dysfunction (46). Spinal cord injury affects ~450,000 United States citizens, with 10,000 new cases annually. Hindbrain abnormalities give rise to orofacial dyskinesia, bruxism, and dysphagia, which contribute to chronic craniofacial maladies (47). Treatment strategies will benefit from more thorough knowledge of spinal cord and brainstem pattern-generating circuitry. This type of lesioning approach will advance our general understanding of the structure and function of CPGs by examining the respiratory oscillator (preBötC) as a model system.

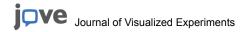
Our lesioning system offers several new advantages. First, neurons can be deleted in a controlled sequence, rather than wholesale, to simulate graded destruction of networks as may occur in disease. The controlled sequence of the ablations is user- and application-specific, and can be based on any number of optically measurable or quantifiable criteria, e.g., in a random sequence, based on centroid position in a volume, as a function of fluorescence signal intensity, as well as other options. In addition, while contemporary optogenetic methods (48,49) allow for selective activation or de-activation of neurons with single-cell precision, the cells do not remain activated or de-activated. Thus, when studying a network behavior like rhythm generation, a ubiquitous brain activity, our approach may provide a useful tool to complement optogenetic methods because single cells can be de-activated cumulatively.

Disclosures

No conflicts of interest declared.

References

1. Feldman JL & Del Negro CA (2006) Looking for inspiration: new perspectives on respiratory rhythm. Nat Rev Neurosci 7(3):232-242.



- Smith JC, Ellenberger HH, Ballanyi K, Richter DW, & Feldman JL (1991) Pre-B tzinger complex: a brainstem region that may generate respiratory rhythm in mammals. Science 254(5032):726-729.
- 3. Inoue S & Spring KR (1997) Video microscopy: the fundamentals (Plenum Press, New York) 2nd Ed pp xx, 741 p., [746] p. of plates.
- 4. Blessing WW (1997) The lower brainstem and bodily homeostasis (Oxford University Press, New York) pp xiv, 575 p.
- 5. Feldman JL (1986) Neurophysiology of breathing in mammals. Handbook of Physiology; Section I: The Nervous System; Volume IV: Intrinsic Regulatory Systems of the Brain., ed Bloom FE (Am. Physiol. Soc., Bethesda, MD), Vol IV, pp 463-524.
- 6. Smith JC, Greer JJ, Liu GS, & Feldman JL (1990) Neural mechanisms generating respiratory pattern in mammalian brain stem-spinal cord in vitro. I. Spatiotemporal patterns of motor and medullary neuron activity. J Neurophysiol 64(4):1149-1169.
- 7. Suzue T (1984) Respiratory rhythm generation in the in vitro brain stem-spinal cord preparation of the neonatal rat. J Physiol 354:173-183.
- 8. Ruangkittisakul A, Schwarzacher SW, Secchia L, Poon BY, Ma Y, Funk GD, & Ballanyi K (2006) High sensitivity to neuromodulator-activated signaling pathways at physiological [K+] of confocally imaged respiratory center neurons in on-line-calibrated newborn rat brainstem slices. J Neurosci 26(46):11870-11880.
- 9. Pierani A, Moran-Rivard L, Sunshine MJ, Littman DR, Goulding M, & Jessell TM (2001) Control of interneuron fate in the developing spinal cord by the progenitor homeodomain protein Dbx1. Neuron 29(2):367-384.
- 10. Hirata T, Li P, Lanuza GM, Cocas LA, Huntsman MM, & Corbin JG (2009) Identification of distinct telencephalic progenitor pools for neuronal diversity in the amygdala. Nat Neurosci 12(2):141-149.
- 11. Glasgow SM, Henke RM, Macdonald RJ, Wright CV, & Johnson JE (2005) Ptf1a determines GABAergic over glutamatergic neuronal cell fate in the spinal cord dorsal horn. Development 132(24):5461-5469.
- 12. Gray PA (2008) Transcription factors and the genetic organization of brain stem respiratory neurons. J Appl Physiol 104(5):1513-1521.
- 13. Gray PA, Janczewski WA, Mellen N, McCrimmon DR, & Feldman JL (2001) Normal breathing requires preB tzinger complex neurokinin-1 receptor-expressing neurons. Nat Neurosci 4(9):927-930.
- 14. Gray PA, Rekling JC, Bocchiaro CM, & Feldman JL (1999) Modulation of respiratory frequency by peptidergic input to rhythmogenic neurons in the preB tzinger complex. Science 286(5444):1566-1568.
- 15. Tan W, Janczewski WA, Yang P, Shao XM, Callaway EM, & Feldman JL (2008) Silencing preBotzinger Complex somatostatin-expressing neurons induces persistent apnea in awake rat. Nat Neurosci 11(5):538-540.
- 16. Winter SM, Fresemann J, Schnell C, Oku Y, Hirrlinger J, & Hulsmann S (2009) Glycinergic interneurons are functionally integrated into the inspiratory network of mouse medullary slices. Pflugers Arch 458(3):459-469.
- 17. Brockhaus J & Ballanyi K (1998) Synaptic inhibition in the isolated respiratory network of neonatal rats. Eur J Neurosci 10(12):3823-3839.
- 18. Feldman JL & Smith JC (1989) Cellular mechanisms underlying modulation of breathing pattern in mammals. Ann N Y Acad Sci 563:114-130.
- 19. Shao XM & Feldman JL (1997) Respiratory rhythm generation and synaptic inhibition of expiratory neurons in pre-Botzinger complex: differential roles of glycinergic and GABAergic neural transmission. J Neurophysiol 77(4):1853-1860.
- 20. Funk GD, Smith JC, & Feldman JL (1993) Generation and transmission of respiratory oscillations in medullary slices: role of excitatory amino acids. J Neurophysiol 70(4):1497-1515.
- 21. Ge Q & Feldman JL (1998) AMPA receptor activation and phosphatase inhibition affect neonatal rat respiratory rhythm generation. J Physiol 509 (Pt 1):255-266.
- 22. Greer JJ, Smith JC, & Feldman JL (1991) Role of excitatory amino acids in the generation and transmission of respiratory drive in neonatal rat. J Physiol 437:727-749.
- 23. Ireland MF, Lenal FC, Lorier AR, Loomes DE, Adachi T, Alvares TS, Greer JJ, & Funk GD (2008) Distinct receptors underlie glutamatergic signalling in inspiratory rhythm-generating networks and motor output pathways in neonatal rat. J Physiol 586(9):2357-2370.
- Wallen-Mackenzie A, Gezelius H, Thoby-Brisson M, Nygard A, Enjin A, Fujiyama F, Fortin G, & Kullander K (2006) Vesicular glutamate transporter 2 is required for central respiratory rhythm generation but not for locomotor central pattern generation. J Neurosci 26(47):12294-12307.
- 25. Guyenet PG, Sevigny CP, Weston MC, & Stornetta RL (2002) Neurokinin-1 receptor-expressing cells of the ventral respiratory group are functionally heterogeneous and predominantly glutamatergic. J Neurosci 22(9):3806-3816.
- 26. Guyenet PG & Wang H (2001) Pre-B tzinger neurons with preinspiratory discharges "in vivo" express NK1 receptors in the rat. J Neurophysiol 86(1):438-446.
- 27. Stornetta RL, Rosin DL, Wang H, Sevigny CP, Weston MC, & Guyenet PG (2003) A group of glutamatergic interneurons expressing high levels of both neurokinin-1 receptors and somatostatin identifies the region of the pre-B tzinger complex. J Comp Neurol 455(4):499-512.
- 28. Stornetta RL, Sevigny CP, & Guyenet PG (2003) Inspiratory augmenting bulbospinal neurons express both glutamatergic and enkephalinergic phenotypes. J Comp Neurol 455(1):113-124.
- 29. Wang H, Stornetta RL, Rosin DL, & Guyenet PG (2001) Neurokinin-1 receptor-immunoreactive neurons of the ventral respiratory group in the rat. J Comp Neurol 434(2):128-146.
- Hayes JA & Del Negro CA (2007) Neurokinin Receptor-Expressing PreB tzinger Complex Neurons in Neonatal Mice Studied In Vitro. J Neurophysiol 97(6):4215-4224.
- 31. Pena F & Ramirez JM (2004) Substance P-mediated modulation of pacemaker properties in the mammalian respiratory network. J Neurosci 24(34):7549-7556.
- 32. Ptak K, Yamanishi T, Aungst J, Milescu LS, Zhang R, Richerson GB, & Smith JC (2009) Raphe neurons stimulate respiratory circuit activity by multiple mechanisms via endogenously released serotonin and substance P. J Neurosci 29(12):3720-3737.
- 33. Rekling JC, Champagnat J, & Denavit-Saubie M (1996) Thyrotropin-releasing hormone (TRH) depolarizes a subset of inspiratory neurons in the newborn mouse brain stem in vitro. J Neurophysiol 75(2):811-819.
- 34. Goulding M (2009) Circuits controlling vertebrate locomotion: moving in a new direction. Nat Rev Neurosci 10(7):507-518.
- 35. Goulding M & Pfaff SL (2005) Development of circuits that generate simple rhythmic behaviors in vertebrates. Curr Opin Neurobiol 15(1):14-20.
- 36. McKay LC, Janczewski WA, & Feldman JL (2005) Sleep-disordered breathing after targeted ablation of preBotzinger complex neurons. Nat Neurosci 8(9):1142-1144.
- 37. Benarroch EE (2003) Brainstem in multiple system atrophy: clinicopathological correlations. (Translated from eng) Cell Mol Neurobiol 23(4-5):519-526 (in eng).
- 38. Benarroch EE, Schmeichel AM, Low PA, & Parisi JE (2003) Depletion of ventromedullary NK-1 receptor-immunoreactive neurons in multiple system atrophy. (Translated from eng) Brain 126(Pt 10):2183-2190 (in eng).



- 39. Maria B, Sophia S, Michalis M, Charalampos L, Andreas P, John ME, & Nikolaos SM (2003) Sleep breathing disorders in patients with idiopathic Parkinson's disease. (Translated from eng) Respir Med 97(10):1151-1157 (in eng).
- 40. Paterson DS, Trachtenberg FL, Thompson EG, Belliveau RA, Beggs AH, Darnall R, Chadwick AE, Krous HF, & Kinney HC (2006) Multiple serotonergic brainstem abnormalities in sudden infant death syndrome. (Translated from eng) JAMA 296(17):2124-2132 (in eng).
- 41. Vetrugno R, Lugaresi E, Plazzi G, Provini F, D'Angelo R, & Montagna P (2007) Catathrenia (nocturnal groaning): an abnormal respiratory pattern during sleep. Eur J Neurol 14(11):1236-1243.
- 42. Alheid GF, Gray PA, Jiang MC, Feldman JL, & McCrimmon DR (2002) Parvalbumin in respiratory neurons of the ventrolateral medulla of the adult rat. J Neurocytol 31(8-9):693-717.
- 43. Alexianu ME, Ho BK, Mohamed AH, La Bella V, Smith RG, & Appel SH (1994) The role of calcium-binding proteins in selective motoneuron vulnerability in amyotrophic lateral sclerosis. (Translated from eng) Ann Neurol 36(6):846-858 (in eng).
- 44. Grillner S (2006) Biological pattern generation: the cellular and computational logic of networks in motion. Neuron 52(5):751-766.
- 45. Kiehn O (2006) Locomotor circuits in the mammalian spinal cord. Annu Rev Neurosci 29:279-306.
- 46. Evans RW (2006) Neurology and trauma (Oxford University Press, New York) 2nd Ed pp xix, 802 p.
- 47. Linden RWA (1998) The scientific basis of eating: taste and smell, salivation, mastication and swallowing, and their dysfunctions (Karger, Basel; New York) pp vii, 244 p.
- 48. Zhang F, Wang LP, Brauner M, Liewald JF, Kay K, Watzke N, Wood PG, Bamberg E, Nagel G, Gottschalk A, & Deisseroth K (2007) Multimodal fast optical interrogation of neural circuitry. Nature 446(7136):633-639.
- 49. Chow BY, Han X, Dobry AS, Qian X, Chuong AS, Li M, Henninger MA, Belfort GM, Lin Y, Monahan PE, & Boyden ES (2010) High-performance genetically targetable optical neural silencing by light-driven proton pumps. Nature 463(7277):98-102.